Available online at www.sciencedirect.com
SCIENCE DIRECT®
Journal of Magnetic Resonance 167 (2004) 56–67
JMR Journal of Magnetic Resonance
www.elsevier.com/locate/jmr

Gaussian approximation in the theory of MR signal formation in the presence of structure-specific magnetic field inhomogeneities. Effects of impermeable susceptibility inclusions

Alexander L. Sukstanskii and Dmitriy A. Yablonskiy*

Mallinckrodt Institute of Radiology, Washington University, St. Louis, MO 63110, USA

Received 29 May 2003; revised 11 November 2003

Abstract

A detailed theoretical description of the signal formation in the presence of mesoscopic structure-specific magnetic field inhomogeneities is presented in the framework of the Gaussian phase distribution approximation for two geometrical models of the field inhomogeneity sources—impermeable spheres and infinitely long cylinders. Analytical expressions for free induction decay (FID) and spin echo (SE) signal attenuation functions $\Gamma(t) \sim -\ln S(t)$ are obtained and comparison with the case of unrestricted diffusion (susceptibility inclusions with freely permeable surfaces) is provided. For short times, the leading term in the FID signal attenuation function is proportional to t^2 similar to the case of unrestricted diffusion; the next term behaves as t^3 as compared to $t^{5/2}$ for the "permeable" case. For the SE signal, the leading term is proportional to t^3 as compared to $t^{5/2}$ for unrestricted diffusion. It is shown that the t^3 approximation can be used for an adequate description of the SE signal only for extremely short times compared to a characteristic diffusion time. In the long-time limit, the attenuation function in the impermeable and permeable sphere model contains not only terms linear in time, but also important terms proportional to $t^{1/2}$. In the cylindrical geometry, the leading term in the long-time expansion of the attenuation function is proportional to $t \ln t$ for both the permeable and impermeable models. Application to description of MR signal in biological tissues in the presence of blood vessel networks and contrast agents is discussed. The validity criterion of the Gaussian approximation is also proposed.

Keywords: Magnetic resonance; Relaxation effects; fMRI; MR contrast agent; Blood vessel network

1. Introduction

In a previous paper [1], the MR signal formation in the presence of structure-specific magnetic field inhomogeneities was analyzed in the case of unrestricted diffusion, in which the surfaces of the magnetized objects inducing the mesoscopic field inhomogeneities were considered to be freely permeable for diffusing spins. The problem was analyzed in the framework of a model, according to which the magnetized objects (blood capillaries, red blood cells, etc.) occupying a small volume fraction ζ (diluted system) with a magnetic susceptibility χ_i are embedded in a given medium (tissue matrix) with a magnetic susceptibility χ_e. General results have been obtained for objects of arbitrary geometry and explicit expressions for MR signal time dependence have been found for some specific geometries of the objects.

However, in many real situations the surfaces of the magnetized objects are not permeable to nuclear spins. Typical examples include superparamagnetic contrast agents, the venous blood vessel network in the brain or muscles, containing deoxygenated blood as a source of inhomogeneous field. Therefore, a theory of MR signal formation in such systems should account for this fact, and this is the aim of the present study. As in [1], the signal will be analyzed in the Gaussian approximation for phases accumulated by diffusing spins. In the case of unrestricted diffusion, where the solution of the diffusion equation is well known, some general expressions for the correlation and signal attenuation functions (see below) are available for an arbitrary shape of the objects.

* Corresponding author. Fax: 1-314-362-0526.
E-mail address: yablonskiyd@mir.wustl.edu (D.A. Yablonskiy).

1090-7807/$ - see front matter © 2003 Elsevier Inc. All rights reserved.
doi:10.1016/j.jmr.2003.11.006

In contrast, when the objects' surfaces are impermeable for spins diffusing outside the objects, the solution of the diffusion equation depends on the specific geometry of the objects through boundary conditions at these surfaces. Hence, the problem should be solved for each objects' geometry separately. In the present paper, we provide such a solution for spherical and cylindrical objects.

As the objects' surfaces are impermeable for diffusing spins, all the spins can be divided into two pools that do not mix with each other and the total signal is a sum of internal, S_i, and external, S_e, parts:

$$S(t) = S_i(t) + S_e(t). \tag{1}$$

The signal S_i for the case of randomly oriented ellipsoids of revolution (spheroids) was found in [2] and will be briefly discussed here. The ''outer sphere'' model, when spins diffuse outside impermeable spheres, has been analyzed in [3,4] in the context of dipolar interaction between diffusing spins (the correlation function $G(t)$ and its Fourier transformation (spectral density) have been found). In what follows, we present explicit expressions for the MR signal time dependence in two models of impermeable magnetized objects: spheres and infinitely long cylinders. Besides, numerical simulations of the signal are made and a validity criterion of the Gaussian approximation is proposed. The theory is applied for describing the MR signal in biological tissues in the presence of blood vessel network and superparamagnetic contrast agents.

2. General approach (external pool)

In the Gaussian approximation (the framework has been discussed in [1]), the MR signal from the spins diffusing in an inhomogeneous magnetic field induced by randomly distributed and randomly oriented magnetized objects can be written in the form

$$S_e(t) = S_{0e}(t)s(t), \quad s(t) = \exp[-\Gamma(t)], \tag{2}$$

where the factor $S_{0e}(t)$ describes the signal time dependence from the external pool of spins in the absence of magnetic field inhomogeneities; the function $\Gamma(t)$, which will be referred to as a signal attenuation function, describes the signal attenuation due to the presence of magnetized objects. For the FID signal (experiment with a single 90° RF pulse followed by a readout period t) and the SE signal (experiment with 90°–t/2–180°–t/2-signal) the signal attenuation functions are:

$$\begin{aligned} \Gamma_{\mathrm{FID}}(t) &= \int_0^t \mathrm{d}\tau(t-\tau)G(\tau), \\ \Gamma_{\mathrm{SE}}(t) &= \int_0^t \mathrm{d}\tau(t-\tau)[G(\tau/2) - G(\tau)]. \end{aligned} \tag{3}$$

Here $G(t)$ is the frequency correlation function. For a uniform initial distribution of molecules diffusing outside the objects,

$$G(t) = \frac{1}{V_e}\left\langle \int\int_{V_e} \mathrm{d}\mathbf{r}\,\mathrm{d}\mathbf{r}_0\,\omega(\mathbf{r})\omega(\mathbf{r}_0)P(\mathbf{r},\mathbf{r}_0,t)\right\rangle. \tag{4}$$

The integration in Eq. (4) is over the volume of the external pool V_e, the angular brackets in Eq. (4) mean averaging over all possible positions and orientations of the objects, $\omega(\mathbf{r}) = \gamma H(\mathbf{r})$ is the local NMR frequency at the position $\mathbf{r}$, γ is the nuclear gyromagnetic ratio, $H(\mathbf{r})$ is the projection of the local nuclear magnetic field $\mathbf{H}(\mathbf{r})$ onto the direction of the external field $\mathbf{H}_0$. In the Lorentzian approximation (see, e.g. [5]), which is fairly precise for isotropic liquids, $\mathbf{H}(\mathbf{r}) = \mathbf{H}_0(1 + 4\pi\chi_e/3) + \mathbf{h}(\mathbf{r})$ in the medium and $\mathbf{H}(\mathbf{r}) = \mathbf{H}_0(1 + 4\pi\chi_i/3) + \mathbf{h}(\mathbf{r})$ inside the objects (we assume that the magnetic susceptibilities $\chi_{i,e}$ are small enough to ignore effects non-linear in χ). In what follows, the frequency $\omega_0 = \gamma H_0(1 + 4\pi\chi_e/3)$ will be considered as the frequency of the rotating frame, and all results will be presented with respect to this reference frequency. In fact, the system under consideration can be treated as a system consisting of the magnetized objects with a relative susceptibility $\Delta\chi = \chi_i - \chi_e$ embedded in a non-magnetic medium with $\chi = 0$. The Lorentz field in this approach differs from zero only within the objects and is equal to $4\pi\Delta\chi\mathbf{H}_0/3$. An inhomogeneous mesoscopic magnetic field $\mathbf{h}(\mathbf{r})$ is induced by all the magnetized objects:

$$\mathbf{h}(\mathbf{r}) = \sum_{n=1}^{N} \mathbf{h}_n(\mathbf{r} - \mathbf{R}_n), \tag{5}$$

where $\mathbf{h}_n$ is the magnetic field induced by the nth object, $n = 1, 2, \ldots, N$, located at the point $\mathbf{R}_n$. The propagator $P(\mathbf{r}, \mathbf{r}_0, t)$ satisfies the diffusion equation

$$\partial P/\partial t = D \cdot \nabla^2 P \tag{6}$$

with the initial condition $P(\mathbf{r}, \mathbf{r}_0, 0) = \delta(\mathbf{r} - \mathbf{r}_0)$ (D is the diffusion coefficient). In the case of diffusion restricted by the objects' surfaces, the diffusion equation (6) should be complemented by boundary conditions on the surfaces. For reflecting and non-depolarizing boundaries, as we assume here, these conditions are

$$(\partial P/\partial \mathbf{n})_s = 0, \tag{7}$$

where $(\partial/\partial\mathbf{n})_s$ means a normal derivative at the object's surface.

For the case of a small volume fraction $\zeta \ll 1$ of the magnetized objects, averaging over objects' positions reduces Eq. (4) to [1]

$$G(t) = \frac{\gamma^2\zeta}{v_0}\left\langle \int\int_{V_e} \mathrm{d}\mathbf{r}\,\mathrm{d}\mathbf{r}_0\,P(\mathbf{r},\mathbf{r}_0,t)\cdot h(\mathbf{r})h(\mathbf{r}_0)\right\rangle_{\text{orientation}}, \tag{8}$$

where the magnetic field $\mathbf{h}(\mathbf{r})$ and the propagator $P(\mathbf{r}, \mathbf{r}_0, t)$ should be calculated in the presence of only a single magnetized object (v_0 is its volume). The solution of the diffusion equation (6) with boundary conditions (7) is different for different geometries and requires

separate considerations. In what follows, we analyze two geometries: spheres and infinitely long cylinders.

3. Impermeable spheres (external pool)

In this model, spins diffuse in the space between randomly distributed spheres of radius R. For an isolated sphere, the solution of the diffusion equation for the propagator $P(\mathbf{r},\mathbf{r}_0,t)$, with boundary condition on the sphere surface corresponding to impermeable surfaces, as well as the Laplace transform $\bar{G}(p)$ of the correlation function have been found in [3]. In our notation

$$\bar{G}(p) = G_0 \cdot \frac{R^2}{D} \cdot \frac{(4+x)}{(9+9x+4x^2+x^3)}, \tag{9}$$

where $x = (p/D)^{1/2}R$ and

$$G_0 = G(0) = \frac{4\zeta(\delta\omega_s)^2}{45}, \quad \delta\omega_s = 4\pi\gamma\Delta\chi H_0. \tag{10}$$

Performing the inverse Laplace transformation, the correlation function $G(t)$ can be written in the form

$$G(t) = G_0 \cdot \sum_{k=1}^{3} A_k \exp\left(\tau x_k^2\right)\tilde{\Phi}\left(-x_k\tau^{1/2}\right), \tag{11}$$

where $\tilde{\Phi}(x) = 1 - \Phi(x)$, $\Phi(x)$ is the error function [6], $\tau = t/t_D$, $t_D = R^2/D$ is the characteristic diffusion time; x_k, $k = 1,2,3$, are the roots of the cubic equation $9 + 9x + 4x^2 + x^3 = 0$, and

$$A_k = \frac{x_k(4+x_k)}{(9+8x_k+3x_k^2)}. \tag{12}$$

An equivalent form of the correlation function in the outer sphere model has been obtained in [4]. Approximate values of the roots x_k and the coefficients A_k are:

$$\begin{aligned} &x_1 \approx -1.783, \quad x_2 = x_3^* \approx -1.108 + 1.954\,\mathrm{i},\\ &A_1 \approx -0.925, \quad A_2 = A_3^* \approx 0.962 - 0.124\,\mathrm{i}. \end{aligned} \tag{13}$$

In the short- and long-time limits ($\tau \ll 1$ and $\tau \gg 1$, respectively), the correlation function (11) takes the form:

$$G(t) \simeq G_0 \cdot \begin{cases} 1 - 9\tau + \frac{36}{\pi^{1/2}}\tau^{3/2}, & \tau \ll 1,\\ \frac{1}{6\pi^{1/2}\tau^{3/2}}, & \tau \gg 1. \end{cases} \tag{14}$$

Note that in the long-time limit, the correlation function in the impermeable sphere model coincides with that obtained in [1,7] for the spherical model in the case of unrestricted diffusion.

Substituting the correlation function (11) in Eq. (3), the external pool signal attenuation functions for the FID and SE signals can be written in the form:

$$\Gamma_{FID}(t) = G_0 t_D^2 \cdot \left\{ \frac{4\tau}{9} - \frac{2}{3}\left(\frac{\tau}{\pi}\right)^{1/2} + \frac{11}{81} + \sum_{k=1}^{3} \frac{A_k \exp(\tau x_k^2)}{x_k^4} \cdot \tilde{\Phi}\left(-x_k\tau^{1/2}\right) \right\}, \tag{15}$$

$$\Gamma_{SE}(t) = G_0 t_D^2 \cdot \left\{ \frac{4\tau}{9} - \frac{2(\sqrt{8}-1)}{3}\left(\frac{\tau}{\pi}\right)^{1/2} + \frac{11}{27} + \sum_{k=1}^{3} \frac{A_k}{x_k^4} \cdot \left[4\exp(\tau x_k^2/2)\tilde{\Phi}\left(-x_k(\tau/2)^{1/2}\right) - \exp(\tau x_k^2)\tilde{\Phi}\left(-x_k\tau^{1/2}\right) \right] \right\}. \tag{16}$$

When obtaining Eqs. (14)–(16), we used the identities related x_k and A_k:

$$\begin{aligned} &\sum_{k=1}^{3} A_k = 1, \quad \sum_{k=1}^{3} A_k x_k = \sum_{k=1}^{3} \frac{A_k}{x_k} = 0, \quad \sum_{k=1}^{3} A_k x_k^2 = -9,\\ &\sum_{k=1}^{3} \frac{A_k}{x_k^2} = -\frac{4}{9}, \quad \sum_{k=1}^{3} A_k x_k^3 = 27, \quad \sum_{k=1}^{3} \frac{A_k}{x_k^3} = \frac{1}{3},\\ &\sum_{k=1}^{3} A_k x_k^4 = -27, \quad \sum_{k=1}^{3} \frac{A_k}{x_k^4} = -\frac{11}{81}, \quad \sum_{k=1}^{3} \frac{A_k}{x_k^5} = \frac{1}{27}. \end{aligned} \tag{17}$$

At short times, $t \ll t_D$, Eqs. (15) and (16) reduce to

$$\begin{aligned} \Gamma_{FID}(t) &\simeq G_0 t_D^2 \cdot \left[\frac{1}{2}\tau^2 - \frac{3}{2}\tau^3 + \frac{144}{35\pi^{1/2}}\tau^{7/2} + O(\tau^4) \right],\\ \Gamma_{SE}(t) &\simeq G_0 t_D^2 \cdot \left[\frac{3}{4}\tau^3 - \frac{36(4-\sqrt{2})}{35\pi^{1/2}}\tau^{7/2} + O(\tau^4) \right]. \end{aligned} \tag{18}$$

In the long-time limit, $t \gg t_D$, the contribution of the sums in Eqs. (15) and (16) is proportional to $\sim \tau^{-1/2} \ll 1$; using the identities (17), the external pool attenuation functions reduce to

$$\begin{aligned} \Gamma_{FID}(t) &= G_0 t_D^2 \cdot \left\{ \frac{4\tau}{9} - \frac{2}{3}\left(\frac{\tau}{\pi}\right)^{1/2} + \frac{11}{81} - \frac{1}{27(\pi\tau)^{1/2}} + O(\tau^{-3/2}) \right\},\\ \Gamma_{SE}(t) &= G_0 t_D^2 \cdot \left\{ \frac{4\tau}{9} - \frac{2(\sqrt{8}-1)}{3}\left(\frac{\tau}{\pi}\right)^{1/2} + \frac{11}{27} - \frac{(4\sqrt{2}-1)}{27(\pi\tau)^{1/2}} + O(\tau^{-3/2}) \right\}. \end{aligned} \tag{19}$$

4. Impermeable cylinders (external pool)

In this model, spins diffuse in the space between randomly distributed and randomly oriented infinitely long cylinders of radius R. For an isolated cylinder, the solution to the diffusion equation (6) with boundary conditions corresponding to the impermeable cylinder's surface is provided in Appendix A. The Laplace transform of the correlation function $\bar{G}(p)$ is given by Eq. (A.17). Performing the inverse Laplace transformation,

after some tedious algebra, the correlation function $G(t)$ can be written in the form

$$G(t) = G_0 \cdot \frac{24}{\pi^2} \cdot \int_0^\infty \mathrm{d}x \frac{\exp(-\tau x^2)}{x^5\left[J_2'^2(x) + N_2'^2(x)\right]}, \tag{20}$$

where G_0 is given in Eq. (10), $\tau = t/t_\mathrm{D}$, $t_\mathrm{D} = R^2/D$, $J_2(x)$, and $N_2(x)$ are the Bessel functions of the first and second types, respectively; the prime denotes a derivative with respect to the argument.

In the short- and long-time limits ($\tau \ll 1$ and $\tau \gg 1$, respectively), the correlation function (20) takes the form:

$$G(t) \simeq \frac{3}{4} G_0 \cdot \begin{cases} 1 - 4\tau + \frac{32}{3\pi^{1/2}}\tau^{3/2}, & \tau \ll 1, \\ \frac{1}{4\tau} + \frac{(\ln 4\tau - C - 1)}{32\tau^3}, & \tau \gg 1. \end{cases} \tag{21}$$

Note that the leading terms in the short- and long-time expansion of $G(t)$, Eq. (21), differ from those in the model of unrestricted diffusion with cylindrical objects by the same numerical factor 3/4. Similar to the impermeable sphere model discussed in the previous section, the second term in the short-time expansion of (21) is linear in τ, whereas in the case of unrestricted diffusion it is proportional to $\tau^{1/2}$ [1, Eq. (38)].

Substituting the correlation function (20) in Eq. (3), we obtain the external pool signal attenuation functions $\Gamma(t)$ for the FID and SE signals:

$$\Gamma(t) = G_0 t_\mathrm{D}^2 \cdot \frac{24}{\pi^2} \cdot \int_0^\infty \mathrm{d}u \frac{g(\tau u^2)}{u^9\left[J_2'^2(u) + N_2'^2(u)\right]}, \tag{22}$$

where

$$\begin{aligned} g_\mathrm{FID}(x) &= \exp(-x) + x - 1, \\ g_\mathrm{SE}(x) &= 4\exp(-x/2) - \exp(-x) + x - 3. \end{aligned} \tag{23}$$

At short times, $t \ll t_\mathrm{D}$, the correlation function is described by Eq. (21) and $\Gamma(t)$ reduces to

$$\begin{aligned} \Gamma_\mathrm{FID}(t) &\simeq G_0 t_\mathrm{D}^2 \cdot \left[\frac{3}{8}\tau^2 - \frac{1}{2}\tau^3 + \frac{32}{35\pi^{1/2}}\tau^{7/2} + \mathrm{O}(\tau^4)\right], \\ \Gamma_\mathrm{SE}(t) &\simeq G_0 t_\mathrm{D}^2 \cdot \left[\frac{1}{4}\tau^3 - \frac{8(4-\sqrt{2})}{35\pi^{1/2}}\tau^{7/2} + \mathrm{O}(\tau^4)\right]. \end{aligned} \tag{24}$$

Similar to the impermeable sphere model, the terms proportional to $\tau^{5/2}$ which are characteristic to the case of unrestricted diffusion, are absent and the leading term in the short-time expansion of the SE signal is proportional to τ^3.

In the long-time limit, $t \gg t_\mathrm{D}$, the external pool attenuation functions contain logarithmic terms:

$$\begin{aligned} \Gamma_\mathrm{FID}(t) &= G_0 t_\mathrm{D}^2 \cdot \left[\frac{3}{16}\tau\ln\tau + C_1\tau + C_2 + \mathrm{O}(\tau^{-1})\right], \\ \Gamma_\mathrm{SE}(t) &= G_0 t_\mathrm{D}^2 \cdot \left\{\frac{3}{16}\tau\ln\tau + C_3\tau + 3C_2 + \mathrm{O}(\tau^{-1})\right\}, \end{aligned} \tag{25}$$

where $C_1 \div C_4$ are numerical constants:

$$\begin{aligned} C_1 &= \frac{3(C-1)}{16} + C_4 \approx 0.152, \\ C_3 &= \frac{3(C-1-\ln 4)}{16} + C_4 \approx -0.108, \\ C_2 &= -\frac{12}{\pi^2}\int_0^\infty \frac{\mathrm{d}u}{u^2} \cdot \frac{\mathrm{d}}{\mathrm{d}u}\left[\frac{1}{u^6\left(J_2'^2(u) + N_2'^2(u)\right)}\right] \approx 0.047, \\ C_4 &= -\frac{24}{\pi^2}\int_0^\infty \mathrm{d}u \ln u \cdot \frac{\mathrm{d}}{\mathrm{d}u}\left[\frac{1}{u^6\left(J_2'^2(u) + N_2'^2(u)\right)}\right] \approx 0.231 \end{aligned} \tag{26}$$

and $C \approx 0.577$ is Euler's constant.

5. Internal pool signal

Generally speaking, in the case of impermeable objects, the internal pool can also contribute to the MR signal. Spheres and infinitely long cylinders are particular cases of ellipsoids of revolution. The internal magnetic field $\mathbf{H}_\mathrm{i}$, induced by the external field $\mathbf{H}_0$ within the ellipsoids, is known to be uniform (effects of the inhomogeneous magnetic field induced by other magnetized objects are of the second order in ζ and are ignored here) and dependent on an orientation of the ellipsoid's principal axes with respect to $\mathbf{H}_0$. Hence, although the internal signal from any given ellipsoid does not decay (aside from the T_2^* relaxation), the total internal signal S_i from a set of ellipsoids with different orientations attenuates in a FID experiment—a powder-distribution-type effect. For uniformly distributed and oriented spheroids, the internal signal has been found in [2]:

$$\begin{aligned} S_\mathrm{i}(t) &= S_{0\mathrm{i}}(t) \cdot s_\mathrm{i}(t), \\ s_\mathrm{i}(t) &= \left(\frac{\pi}{2|\lambda|}\right)^{1/2} \cdot \exp\left(\mathrm{i}\frac{\lambda}{3}\right) \cdot \left[C(|\lambda|^{1/2}) - \mathrm{i}\,\mathrm{sgn}(\lambda) S(|\lambda|^{1/2})\right], \end{aligned} \tag{27}$$

where $S_{0\mathrm{i}}(t)$ describes the signal time dependence due to the intrinsic T_2^* relaxation, $\lambda = (\delta\omega_\mathrm{s} t)(n_z - n_x)$, $\delta\omega_\mathrm{s}$ is given in Eq. (10), n_z and n_x are demagnetizing factors of the spheroid along its principal axis and perpendicular to it, respectively, $C(x)$ and $S(x)$ are Fresnel functions (e.g. [6]). In the short- and long-time limits, Eq. (27) reduces to[1]

$$s_\mathrm{i} \approx \begin{cases} 1 - \frac{2}{45}\lambda^2 + \mathrm{i}\frac{8}{2835}\lambda^3, & \lambda \ll 1, \\ \frac{1}{2}\left(\frac{\pi}{|\lambda|}\right)^{1/2} \exp\left[\mathrm{i}\cdot\left(\frac{\lambda}{3} - \frac{\pi}{4}\mathrm{sgn}\lambda\right)\right], & |\lambda| \gg 1. \end{cases} \tag{28}$$

[1] There is a misprint in Eq. (37) of Ref. [2] for the internal dephasing function s_i: an erroneous factor $\exp(\mathrm{i}p)$ should be substituted by $\exp(\mathrm{i}p/3)$. Expressions for the short- and long-time behavior of s_i are correct.

For spheres, $n_z = n_x = 1/3$, $\lambda \equiv 0$, and $s_i(t) = 1$. This result is expected because orientation averaging for spheres is meaningless and does not lead to signal attenuation. For infinitely long cylinders, $n_z = 0$, $n_x = 1/2$, and the internal signal is given by Eq. (27) with $\lambda = (\delta\omega_s t)/2$.

6. Discussion

In the case of ellipsoidal susceptibility inclusions, the signal from the internal pool, Eq. (27), was discussed in detail in [2]. Here we will concentrate on the discussion of the signal from the external pool only. As mentioned previously, such a separation is possible because in the case of impermeable susceptibility inclusions, spins from internal and external pools do not exchange and contribute to the total signal additively. Besides, for a number of experimental situations, the internal pool gives zero or negligible contribution to the total signal. Examples include ferrite particles when there is no intraparticle water molecules; venous blood vessel networks in which blood signal may be diminished by specially designed experimental protocols that suppress the signal from the moving blood, or reduced due to the very short T_2 relaxation time constant resulting either from high level of deoxyhemoglobin, or high external magnetic field, or high concentration of contrast agent.

The discussion of the external pool signal attenuation function $\Gamma(t)$ will be accompanied by comparison with the case of unrestricted diffusion [1] when the signal decay is characterized by a similar attenuation function $\Gamma^{(0)}(t)$ calculated in the same geometrical models of spherical and cylindrical magnetized objects with freely permeable surfaces (hereafter quantities for the freely diffusing spins are marked by the upper index (0)). Intuitively, one could expect that the difference between functions $\Gamma(t)$ and $\Gamma^{(0)}(t)$ in the case of small volume fraction ζ should vanish as $\zeta \to 0$ because (a) the inhomogeneous magnetic field outside the objects is identical in both the cases and (b) even for freely permeable objects' surfaces, diffusing spins spend very short time (relative time is proportional to $\zeta \ll 1$) within the objects. We will demonstrate however that there are both quantitative and qualitative differences between these two cases.

The time dependence of the functions $\Gamma_{\mathrm{FID}}(t)$ and $\Gamma_{\mathrm{SE}}(t)$ in the model of impermeable spheres (Eqs. (15) and (16)) is shown in Fig. 1 (solid lines). The attenuation functions $\Gamma^{(0)}_{\mathrm{FID}}(t)$ and $\Gamma^{(0)}_{\mathrm{SE}}(t)$ calculated in the same geometrical model of spherical magnetized objects in the case of freely permeable spheres (unrestricted diffusion) [1] are shown by dashed lines. As we see, for both FID and SE signals $\Gamma(t) > \Gamma^{(0)}(t)$, i.e., the signal attenuates stronger in the case of impermeable spheres. This fact can be expected because in the case of unrestricted diffusion, the attenuation functions $\Gamma^{(0)}_{\mathrm{FID}}(t)$ and $\Gamma^{(0)}_{\mathrm{SE}}(t)$

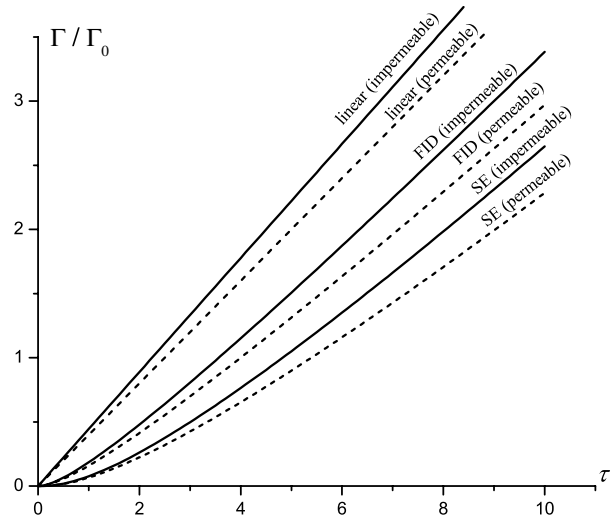

Fig. 1. The attenuation functions $\Gamma(t)$ ($\Gamma = -\ln S/S_0$) for the FID and SE signals as functions of dimensionless time $\tau = t/t_D$ for the cases of impermeable (solid lines) and permeable (dashed lines) spheres. S is the signal from the external pool in the case of impermeable objects and the total signal for permeable objects, both normalized to $\Gamma_0 = G_0 t_D^2 = 4/45 \cdot (4\pi\gamma\Delta\chi H_0)^2 (R^2/D)^2$. Also shown the linear approximations for $\Gamma(t)$ in the long-time regime, corresponding to the mono-exponential ΔR_2 (or ΔR_2^*) relaxation.

describe the "total signal" when the spins spend some time within the spheres, where the local nuclear field is homogeneous and, therefore, during this time their contribution to the signal decay is absent. Hence, the signal in this case decays more weakly than the signal from the external pool in the case of impermeable spheres, where spins all the time diffuse in the inhomogeneous magnetic field outside the spheres.

The time dependence of the functions $\Gamma_{\mathrm{FID}}(t)$ and $\Gamma_{\mathrm{SE}}(t)$ in the model of impermeable cylinders (Eqs. (22) and (23)) is shown in Fig. 2 (solid lines). Dashed lines in Fig. 2 correspond to the attenuation functions $\Gamma^{(0)}_{\mathrm{FID}}(t)$ and $\Gamma^{(0)}_{\mathrm{SE}}(t)$ calculated in the model of permeable cylindrical magnetized objects [1]. Opposite to the spherical model, in the cylindrical model the signal for impermeable objects attenuates more weakly than in the case of unrestricted diffusion: for both the FID and SE signal $\Gamma(t) < \Gamma^{(0)}(t)$. This is due to the role of a powder-distribution-type effect that leads to an additional total signal attenuation in the case of permeable cylinders and does not make any contribution to $\Gamma^{(0)}(t)$ in the case of permeable spheres.

Comparing the short-time behavior of the signals in the model of impermeable spheres (18) and cylinders (21) with the corresponding expansions of $\Gamma^{(0)}(t)$ for the case of unrestricted diffusion (see Eqs. (34) and (41) in [1][2]), one can see that for the FID signal, the leading

[2] The short-time expansions of the SE signal (second lines in Eqs. (34) and (41)) in [1] are given with misprints: the factor $(Dt/R^2)^{5/2}$ should be substituted by $t^{5/2}(D/R^2)^{1/2}$.

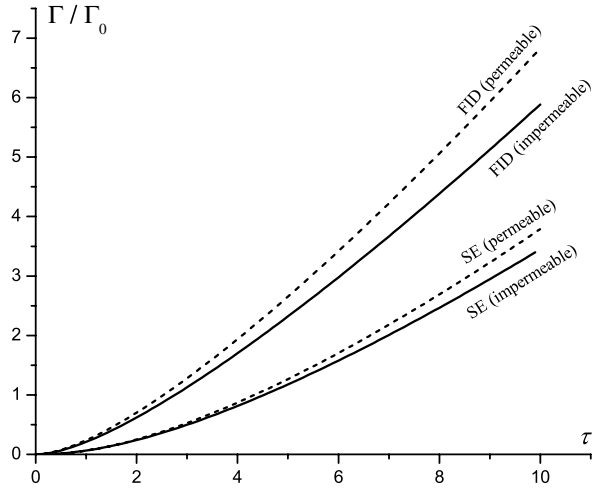

Fig. 2. The attenuation functions $\Gamma(t)$ ($\Gamma = -\ln S/S_0$) for the FID and SE signals as functions of dimensionless time $\tau = t/t_D$ for the cases of impermeable (solid lines) and permeable (dashed lines) infinitely long cylinders. S is the signal from the external pool in the case of impermeable objects and the total signal for permeable objects, normalized to $\Gamma_0 = G_0 t_D^2 = 4/45 \cdot (4\pi\gamma\Delta\chi H_0)^2 (R^2/D)^2$.

term is quadratic in time for both $\Gamma_{FID}(t)$ and $\Gamma^{(0)}_{FID}(t)$. However, the leading terms for the SE signal (and the second terms for the FID signal) are different: t^3 in $\Gamma(t)$ rather than $t^{5/2}$ in $\Gamma^{(0)}(t)$. The origin of the $t^{5/2}$-dependence of the signal attenuation function at short times in the case of unrestricted diffusion was explained in [1]: it is connected with a dominant role of spins crossing the objects' surfaces where the local field is discontinuous and the Larmor frequency has a jump discontinuity. In the impermeable models, spins diffuse only outside the objects and there is no discontinuity in their Larmor frequency. In this situation, the leading term in $\Gamma_{SE}(t)$ demonstrates a "standard" t^3—short-time behavior. In particular, such a t^3 time dependence of the attenuation function can be obtained based on the assumption that at short time, when a spin's displacement is small, its diffusion can be considered as unrestricted diffusion in the constant local field gradients, and the attenuation function for the SE signal is (see, e.g. [8–11]):

$$\tilde{\Gamma}_{SE}(t) = \frac{D}{12}\gamma^2 \langle \nabla h(\mathbf{r}) \rangle^2 t^3. \tag{29}$$

It is easy to verify that Eq. (29) leads (in our notations) to $\tilde{\Gamma}_{SE}(t) = 3G_0 D t^3/4R^2$ for spheres and $\tilde{\Gamma}_{SE}(t) = G_0 D t^3/4R^2$ for cylinders, which exactly coincide with the t^3 terms in the short time expansions of $\Gamma_{SE}(t)$ in Eqs. (18) and (24), respectively. Note, however, that the presence of the impermeable objects hinders spin diffusion near the objects' surfaces. For short time, spins located within the characteristic diffusion distance $(Dt)^{1/2}$ encounter the surfaces, a relative number of such spins being proportional to $(Dt)^{1/2} \cdot (s_0/v_0)$, where (s_0/v_0) is the surface-to-volume ratio (for spheres and cylinders, this ratio is $3/R$ and $2/R$, respectively). This leads to a decrease in effective diffusivity and can be taken into account by substituting the diffusion coefficient D in Eq. (29) by an effective diffusion coefficient $D \to D_{eff} = D[1 - \beta(Dt)^{1/2}/R]$, where β is a geometry-dependent numerical coefficient (a similar short time dependence of the effective diffusion coefficient in porous systems was discussed in [12]). Hence, the restriction of diffusion by the objects' surfaces modifies the t^3 time dependence of $\Gamma_{SE}(t)$ by generating an additional negative term proportional to $-D^{3/2}t^{7/2}/R^3$, as appears in Eqs. (18) and (24). Due to the presence of such a $t^{7/2}$ term, the time interval where the cubic term adequately describes the signal behavior is practically absent. This point is demonstrated in Fig. 3, where a relative error is shown between the exact attenuation function $\Gamma_{SE}(t)$ and the short time approximation including only the t^3 term. Even for $\tau \sim 0.01$, the relative error is already about 20% for the sphere model and about 15% for the cylindrical model, reaching at $\tau \sim 0.1$, 100 and 60%, respectively. This result clearly demonstrates that the t^3-approximation can be used for an adequate description of the SE signal only for extremely short times compared to the characteristic diffusion time t_D.

The leading (linear in time) terms in the long-time expansion of the signal attenuation function in the impermeable sphere model (19) describe a standard mono-exponential ΔR_2-relaxation (ΔR_2^* for the FID signal) with $\Delta R_2 = \Delta R_2^* = 4G_0 t_D/9$, that differs by the numerical factor 9/10 from the corresponding quantity obtained for the case of unrestricted diffusion where $\Delta R_2^{(0)} = \Delta R_2^{*(0)} = 2G_0 t_D/5$ [1,3,7]. This difference was first demonstrated in [3] and reiterated in [13]. It should be mentioned, however, that the second terms in Eq. (19) (proportional to $\tau^{1/2}$) also increase with time and their contribution must be included for correct interpretation of experimental data. Describing experimental

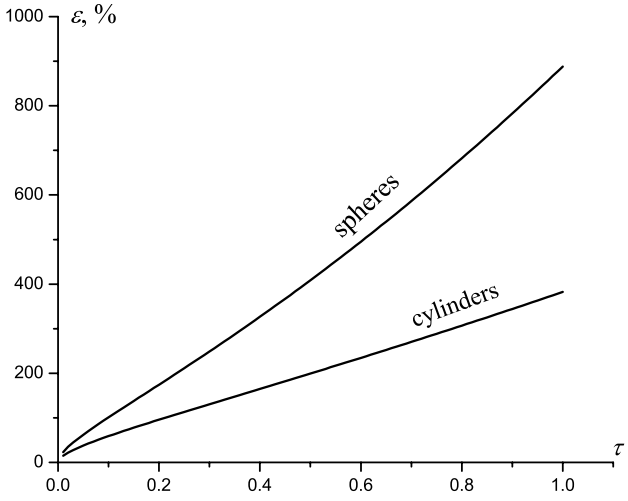

Fig. 3. The relative error between the exact SE signal attenuation function $\Gamma_{SE}(t)$ and the short time approximation $\tilde{\Gamma}_{SE}(t)$ including only t^3 term: $\varepsilon = |\Gamma_{SE} - \tilde{\Gamma}_{SE}|/\Gamma_{SE} \cdot 100\%$.

data for $\Gamma(t)$ in the motional narrowing regime by a linear function may lead to an erroneous value of ΔR_2 (the same situation holds for the case of unrestricted diffusion). The straight lines in Fig. 1 correspond to the linear time dependence of the attenuation functions (with the numerical coefficient 4/9 for $\Gamma(t)$ and 2/5 for $\Gamma^{(0)}(t)$). The $\tau^{1/2}$-terms remain substantial up to very large τ because its relative contribution decreases with time rather slowly ($\sim \tau^{-1/2}$). For instance, even for $\tau = t/t_D = 100$, the difference between an exact result and a linear approximation is still on the order of 10%.

The leading term in the long-time expansion of the attenuation function in the impermeable cylinder model (25) is proportional to $\tau \ln \tau$ and differs from the leading term in the analogous expansion of $\Gamma^{(0)}(t)$ by the factor 3/4 (Eq. (42) in [1]). Similar to the impermeable sphere model, a correct interpretation of experimental data at $\tau \gg 1$ requires accounting for not only this leading term but also for the next term proportional to τ.

6.1. Validity of the Gaussian approximation

The Gaussian approach was first proposed by Douglass and McCall [14] for an analysis of MR signal in the presence of a constant field gradient for the case of unrestricted diffusion when it represents an exact solution to the problem. An adequateness of the Gaussian approximation for different models of restricted diffusion in the case of a constant field gradient was discussed by many authors (see, e.g. [15–20]). If the field gradients are non-uniform (as in the case discussed in the present paper), the phase distribution function is also, in general, not Gaussian. As to our best knowledge, there is no detailed analysis of the validity of the Gaussian phase approximation in such systems.

Generally, the Gaussian approximation is known to be valid in two limiting cases. (A) For short times, when phases accumulated by spins are small, $|\varphi| \ll 1$, and the signal can be approximated by the second cumulant, $s = \langle \exp(i\varphi) \rangle \approx \exp(-\langle \varphi^2 \rangle/2)$. (B) In the motional narrowing regime, when $t \gg t_D$ and the characteristic diffusion time across field inhomogeneities, t_D, is much smaller than the characteristic dephasing time t_c, $t_D \ll t_c$, where we define

$$t_c = (\delta\omega_s/d)^{-1} = \left(\frac{4\pi}{d}\gamma\Delta\chi H_0\right)^{-1} \tag{30}$$

the parameter $d = 3$ in the case of spheres and $d = 2$ for the cylinders. In the case $t_D \ll t_c$, a diffusing spin samples all possible values of the magnetic field prior to the signal substantially decreases. Under this condition, the central limit theorem can be applied that leads to the Gaussian phase distribution. However, a detailed quantitative comparison of the Gaussian approximation with exact results provided in [20] for some models of restricted diffusion in the presence of a constant field gradient demonstrated that in reality, a range of validity of the Gaussian approximation is much broader than the two limiting cases mentioned above. For instance, it was demonstrated that for a SE signal this approximation is adequate for the description of MR signals corresponding to arbitrary relationship between t_D and t_c—the maximum discrepancy between an exact SE signal and that from the Gaussian approximation does not exceed several percent while the signal decays to $1/e$ of its initial value. For the FID signal, the Gaussian approximation is shown to be an adequate for short times and under condition $t_D \leqslant t_c$.

Obviously, in the problem of susceptibility induced magnetic inhomogeneities, the criteria of applicability of the Gaussian approximation in our models should relate not only the characteristic times t_D and t_c but the volume fraction ζ as well. Here we provide results of a numerical analysis of the validity of the Gaussian approximation based on computer (Monte–Carlo) simulation of the MR signal attenuation in the presence of impermeable magnetized inclusions (cylinder or sphere). For simulations, we use two simplified models: a single cylinder of the radius R located in the center of a rectangular box with a square cross section of side $2A$ (the external field H_0 is perpendicular to the cylinder's axis) and a single sphere of the radius R located in the center of a cube $2A$ on edge. For the case of small volume fraction $\zeta \ll 1$, such models are reasonable approximations for more complicated models of uniformly distributed cylinders and spheres described in the main text. The signal dependence on the dimensionless time $\tau = t/t_D$ is completely determined by the volume fraction $\zeta = \pi(R/A)^d/2d$ and the dimensionless parameter

$$p = \frac{t_c}{t_D} = \frac{Dd}{4\pi\gamma\Delta\chi H_0 R^2}. \tag{31}$$

In both the models, the FID and SE signals are calculated for 4 values of the volume fraction $\zeta = 0.03, 0.06, 0.09, 0.12$, and for 5 values of the parameter $p = 0.02$, 0.05, 0.1, 0.3, and 0.5. An exact time dependence of the simulated FID and SE signals is compared to its Gaussian approximation.

The time interval $0 \leqslant \tau \leqslant \tau^*$, where τ^* is time when the signal has decayed by $1/e$, $s(\tau^*) = e^{-1}$, is of the most interest from practical point of view. The simulations show that the discrepancy between the exact time dependence of the signal $s(\tau)$ and its Gaussian approximation $s^{(G)}(\tau)$ within this interval monotonically decreases with the volume fraction and/or the parameter p increase. Note also that the signal calculated in the Gaussian approximation is smaller than the real one, $s^{(G)}(\tau) < s(\tau)$.

To obtain a quantitative criterion of the validity of the Gaussian approximation, we estimate a "proximity" of the Gaussian approximation $s^{(G)}(\tau)$ to the exact signal $s(\tau)$. A numerical quantity determining this proximity is the mean square relative error $\bar{\varepsilon}$ between the curves

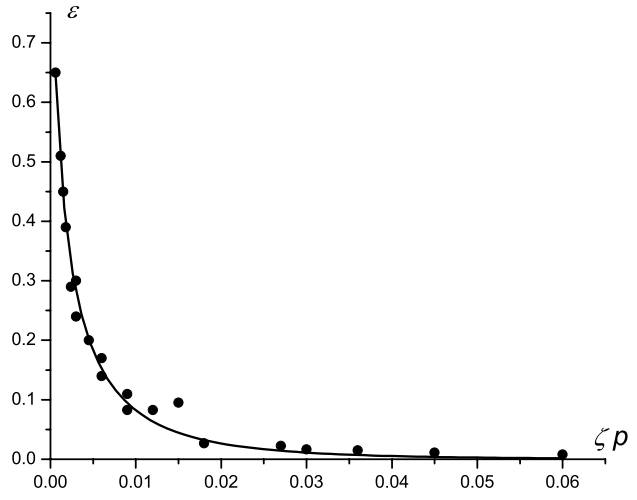

Fig. 4. The mean square relative error $\bar{\varepsilon}$ between the simulated FID signal $s(\tau)$ and its Gaussian approximation $s^{(G)}(\tau)$ in the sphere model as a function of the parameter $\zeta \cdot p$ (dots). The solid line represents the interpolation function (33).

$$\bar{\varepsilon} = \left(\frac{1}{n} \sum_{j=1}^{n} \varepsilon_j^2 \right)^{1/2}, \quad \varepsilon_j = \frac{\left(s(\tau_j) - s^{(G)}(\tau_j) \right)}{s(\tau_j)}, \tag{32}$$

where $\tau_j = j\tau^*/n$, $j = 1, 2, \ldots, n$ is a set of equidistant points on the interval $(0, \tau^*)$. An analysis shows that, in fact, the quantity $\bar{\varepsilon}$ can be well described as a function of product $\zeta \cdot p$. As an example, the function $\bar{\varepsilon} = \bar{\varepsilon}(\zeta \cdot p)$ for the FID signal generated for the sphere model is shown in Fig. 4 (dots). The numerically found dependence $\bar{\varepsilon} = \bar{\varepsilon}(\zeta \cdot p)$ is pretty well interpolated by the exponential function (solid line),[3]

$$\begin{aligned} \bar{\varepsilon}(\beta) &\simeq A \exp[-k \cdot (\zeta \cdot p)^{1/2}] \\ &= A \exp\left[-k \cdot \left(\frac{\zeta D d}{4\pi\gamma \Delta\chi H_0 R^2} \right)^{1/2} \right], \end{aligned} \tag{33}$$

where $A \approx 1.25$ and $k \approx 27$. For the SE signal in the sphere model and the FID and SE signal in cylinder model, the dependence $\bar{\varepsilon} = \bar{\varepsilon}(\zeta \cdot p)$ is similar to Eq. (33) with slightly different numerical parameters A and k.

Thus, we can infer that the discrepancy between the exact signal and its Gaussian approximation exponentially fast decreases with the parameter $\zeta \cdot p$ increases and the qualitative criterion of the validity of the Gaussian approximation is $\bar{\varepsilon} \ll 1$, that requires

$$\zeta \cdot p = \frac{\zeta D d}{4\pi\gamma \Delta\chi H_0 R^2} > 1. \tag{34}$$

Note, however, that the coefficient k in Eq. (33) is not small, $k \approx 27$. Therefore, if we are interested in an accuracy of the Gaussian approximation up to 10%, for instance, the criterion (34) becomes substantially "softer": the Gaussian approximation describes the exact signal on the interval $(0, \tau^*)$ if

$$\begin{aligned} &\zeta \cdot p > 0.01 \text{ (accuracy 10\%)}, \\ &\zeta \cdot p > 0.02 \text{ (accuracy 5\%)}. \end{aligned} \tag{35}$$

It is interesting to compare the validity criterion of the Gaussian approximation (34) with that of the static dephasing regime [21]: $p \ll 1$ for cylinders and $p \ll \zeta^{-1/3}$ for spheres (in our notations). As shown experimentally by Bowen et al. [22], the static dephasing regime actually takes place under "soft" condition $p < \zeta^{-1/3}$ (for spheres). It is easy to see that for $\zeta \sim 1$ the validity criteria of the Gaussian approximation and for the static dephasing regime are just opposite to each other. If $\zeta \ll 1$, there exists an interval $\zeta^{-1/3} < p < \zeta^{-1}$, where neither the Gaussian approximation nor the static dephasing regime is valid. Note, however, that if the "soft" criterion of the Gaussian approximation is used, $\zeta \cdot p > 0.01$, the intervals of validity of the Gaussian approximation and the static dephasing regime could overlap. It is also worth noting that in the Gaussian regime and for $t \gg t_D$, the signal decays mono-exponentially (Eq. (19)) with the relaxation rate $\Delta R_2 = \Delta R_2^* \sim \zeta t_D / t_c^2 = \zeta / p t_c$. Whereas in the static dephasing regime, $\Delta R_2^* \sim \zeta / t_c$ [21]. Consequently, in the static dephasing regime when $t_D > t_c$, the relaxation process goes faster than in the regime when the Gaussian approximation is valid.

The inequality (34) can be considered in two ways. First, for the volume fraction (and other parameters) fixed, it puts an upper limit for the inclusions' radius R:

$$R < \left(\frac{\zeta D d}{4\pi\gamma \Delta\chi H_0} \right)^{1/2}. \tag{36}$$

If the inequality does not hold, the transition from the Gaussian approximation to the static dephasing regime should be expected. The validity of the static dephasing regime [21] for sufficiently large radii of the inclusions was numerically confirmed by Weisskoff et al. [23] and Boxerman et al. [24] and experimentally by Bowen et al. [22]. As the criteria of the Gaussian approximation and the static dephasing regime are, to some extent, opposite to each other, these studies implicitly confirm the statement that the Gaussian approximation fails for large radii of the magnetized inclusion.

On the other hand, the inequality (34) put a *lower* limit for the volume fraction if the radius of the inclusion is fixed:

$$\zeta > \frac{4\pi\gamma \Delta\chi H_0 R^2}{D d}. \tag{37}$$

This result can be explained as follows. The inhomogeneous magnetic field induced by a magnetized inclusion rapidly decreases with distance from the inclusion (as

[3] A more detailed analysis shows that, in reality, the dependence of the mean square relative error $\bar{\varepsilon}$ on the parameters ζ and p could be more complicated: $\bar{\varepsilon} \sim \exp(-k\zeta^n p^m)$, where n and m are in the range 0.5–0.8. This issue will be addressed in more detail in a separate publication.

$(r/R)^{-2}$ for cylinders and $(r/R)^{-3}$ for spheres) and spins located far from the inclusion do not contribute to the signal decay. Whereas the Gaussian approximation sets in (apart from the short-time regime) only when all spins have mixed up by diffusion and lost their "individuality" defined by their initial positions. This process requires time $T_D \sim A^2/D \gg t_D$. Moreover, for the sufficiently small volume fraction, T_D turns out to be longer than τ^* and the signal decays by the factor $1/e$ faster than the spins have mixed up.

6.2. Blood vessel network

As an example of a real system, which can be described by the models analyzed above, we consider blood vessels in the brain, which form an interconnected network of long tubes compared to their radii that range from 3 to 5 μm for small capillaries to 10–50 μm and higher for arterioles, veins, etc. A total volume fraction of all blood vessels in the brain parenchyma is on the order 2–4%. The magnetic susceptibility difference between interior of vessels and the surrounding space is caused by paramagnetic deoxyhemoglobin in venous blood, $\Delta\chi = \Delta\chi_0(1 - Y)Hcr$, where $\Delta\chi_0 = 0.27 \times 10^{-6}$ is the susceptibility difference between the cytoplasm of fully oxygenated and fully deoxygenated red blood cells [25], Y is the blood oxygenation level, and Hcr is the hematocrit. The mid-to-large vessels are impermeable for water molecules and therefore their contribution to the signal decay can be considered in the framework of the approach discussed in the present paper. According to the criterion (35), the Gaussian approximation provides the accuracy of 10%, if

$$\zeta p = \frac{\zeta D}{2\pi\gamma\Delta\chi H_0 R^2} > 0.01 \tag{38}$$

(the parameter p is defined in Eq. (31) for cylinders, $d = 2$). Using the following typical values: magnetic field $H_0 = 1.5\,\mathrm{T}$, $\gamma = 2.675 \times 10^8\,(\mathrm{s}\cdot\mathrm{T})^{-1}$ (proton gyromagnetic ratio), venous blood oxygenation level $Y = 0.6$, hematocrit $Hcr = 0.4$, water diffusion coefficient in the brain $D \sim 1\,\mu\mathrm{m}^2/\mathrm{ms}$, volume fraction $\zeta \sim 0.03$, we infer that for these values of the parameters, the Gaussian approximation is valid for vessels with $R \leqslant 5\,\mu\mathrm{m}$. This range of blood vessels' radii corresponds mainly to small capillaries, which are permeable for water molecules; for their description, the approach developed in [1] for the case of free diffusion can be used. As to impermeable mid-to-large blood vessels with $R > 5\,\mu\mathrm{m}$, the Gaussian approximation provides an accuracy of 10% (or better) for lower magnetic fields; in particular, for $H_0 = 0.2\,\mathrm{T}$, the same accuracy of 10% is achieved for $R \leqslant 14\,\mu\mathrm{m}$.

The characteristic diffusion time t_D for blood vessels with $R \sim 10\,\mu\mathrm{m}$ is about 100 ms. Consequently, for $t < 100\,\mathrm{ms}$, the signal attenuation function reveals its short-time behavior (see Eq. (24)), whereas for $t > 100$ ms, the long-time $t \ln t$-asymptotic expressions (25) can be used.

6.3. MR contrast agents

Consider next the applicability of the Gaussian approximation (sphere model) for describing the MR signal in the presence of contrast agents, for instance, superparamagnetic iron oxide nanoparticles. Typical examples include MION and other iron oxide-based nanoparticles [26,27] consisting of a single-crystal inner core containing about $n = 2000$ atoms of Fe organized in the inverse spinel-type lattice, covered by a mean of 20–25 surface bound dextran molecules. A size of MION is about 20 nm in diameter (in aqueous solution), the core size is about 4.6 nm. The configuration of dextran molecules is rather flexible and may allow water diffusion within MION (but outside the core). Thus, from the diffusion point of view, MION can be considered as a impermeable sphere with radius $R \approx 2.3\,\mathrm{nm}$. The characteristic diffusion time for such particles is extremely short (several nanoseconds); for any reasonable time $t \gg t_D$, the attenuation function is linear in time and the signal decay in the Gaussian approximation can be described by the standard relaxation rate (the linear term in the long-time regime, see Eqs. (19)) :

$$\Delta R_2 = \Delta R_2^* = \frac{16}{45}\zeta\frac{t_D}{t_c^2}, \tag{39}$$

where t_c is the characteristic dephasing time defined in Eq. (31) (for spheres $d = 3$). In the presence of a strong enough external magnetic field (>1.5 T), the superparamagnetic MION particles are saturated to their saturation magnetization M, therefore

$$t_c = \frac{3}{4\pi\gamma M} \tag{40}$$

The magnetization M is determined by the number of Fe atoms in the core, an average magnetic moment μ per 1 atom Fe and the core's volume: $M = n\mu/v_0$, $v_0 = 4\pi R^3/3$. The volume fraction ζ can be determined by the molar concentration of Fe in the solution λ: $\zeta = \lambda N_a v_0/n$, $N_a = 6.02 \times 10^{23}\,\mathrm{mol}^{-1}$ is Avogadro's number. Thus, the relaxation rate can be written in the form:

$$\Delta R_2 = \frac{\pi}{15}\left(\frac{8\gamma\mu}{3}\right)^2\frac{\lambda N_a n}{DR}. \tag{41}$$

Experimentally [26], the relaxation rate of MION in the aqueous solution is found to be $\Delta R_2 = 34.8(\mathrm{mM\,s})^{-1}$. Substituting $\gamma = 2.675 \times 10^8\ (\mathrm{s\,T})^{-1}$, $D = 2.5\,\mu\mathrm{m}^2/\mathrm{ms}$, $n = 2064$, $R = 2.3\,\mathrm{nm}$, we estimate the magnetic moment per 1 atom Fe: $\mu = 1.34\mu_B$ ($\mu_B = 0.93 \times 10^{-20}$ erg/Gauss is Bohr's magneton) that is typical for spinel-type ferrites. The corresponding characteristic diffusion and dephasing times are $t_D \approx 2\,\mathrm{ns}$, $t_c \approx 18\,\mathrm{ns}$, and $p = t_c/t_D \approx 9$.

It should be mentioned that for the above estimate we used the radius of the MION core as a particle of radius R assuming water molecules can freely diffuse within the dextran coat. In reality, such diffusion is hindered as compared to the space outside the MION particle and an "apparent" radius R_{app} can be introduced (bigger than the radius of the inner core 2.3 nm but smaller than the external radius of MION 10 nm). According to the validity criterion of the Gaussian approximation, the latter provides the accuracy of 10% if

$$\zeta p = \frac{3\zeta D}{4\pi\gamma M R^2} > 0.01. \tag{42}$$

The inequality (42) put a lower limit for the volume fraction ζ, depending on the parameter p. For $2.3 < R_{app} < 10$ (nm), $9 < p < 19$, the Gaussian approximation is valid (with accuracy to 10%) if $\zeta > (0.5 \div 1) \times 10^{-3}$, or $\lambda > 30 \div 60$ mM.

Another possible experimental situation mentioned above takes place when the volume fraction ζ being fixed whereas the radius R of the magnetized inclusions varies. As applied to nanocompounds, the condition (36) can be re-written as

$$R < \left(\frac{75\zeta D}{\pi\gamma M}\right)^{1/2}. \tag{43}$$

As mentioned above, the characteristic diffusion time t_D for nanoparticles is much shorter than any reasonable experimental time and the signal decays mono-exponentially and can be described by the relaxation rate ΔR_2 (or ΔR_2^*). However, this description fails when nanoparticles are compartmentalized within cells with impermeable for them membranes (or oppositely, nanoparticles are restricted to extracellular space). If the cell concentration is small enough, a cell loaded by nanoparticles should be considered as a single big magnetized "particle." For a cell size $\sim 3\,\mu$m and $D \sim 1\,\mu m^2$/ms, the characteristic diffusion time is $t_D \sim 10$ ms. Recall that even when $t = 100 t_D$, the terms proportional to $t^{1/2}$ in Eq. (19) substantially contribute to the signal attenuation function, the latter is not linear in time and should be described by the general expressions (15) and (16) or their long-time approximations with non-linear terms in t. The short-time behavior of the signal described by Eq. (18) can be observed if $t < t_D$.

For fixed cell's size and volume fraction, the validity condition of the Gaussian approximation (35) (10% accuracy is assumed) puts an upper limit for the average magnetization within a cell $M_c = \zeta M$ (M is the magnetization of nanoparticles, ζ is their volume fraction within a cell):

$$M_c < \frac{75\zeta_c D}{\pi\gamma R_c^2}, \tag{44}$$

where R_c, ζ_c are the cell's size and volume fraction. For instance, for $R_c = 3\,\mu$m, $\zeta_c = 0.01$, $D = 1\,\mu m^2$/ms, M_c should be less than 1 mG. For higher magnetization, the Gaussian approximation is inapplicable and the signal can be described in the framework of the static dephasing regime [21]. This was recently demonstrated by Bowen et al. [22] in experiments, in which superparamagnetic nanoparticles (SHU 555A, SHU 555C) were compartmentalized within THP-1 cells.

7. Conclusion

In the present paper, we provided a detailed description of the FID and SE signals in the models of impermeable spherical and impermeable cylindrical sources of magnetic field inhomogeneities in the framework of the Gaussian phase distribution approximation. The expressions for the frequency correlation functions $G(t)$ and the signal attenuation functions $\Gamma(t)$ are obtained. For short times, the leading term in the FID signal attenuation function is t^2 similar to the case of unrestricted diffusion. However, the next term behaves as t^3 as compared to $t^{5/2}$ for the "permeable" case. For SE signal the leading term is proportional to t^3 in impermeable models as compared to $t^{5/2}$ for unrestricted diffusion. However, the t^3 approximation can be used for an adequate description of the SE signal only for extremely short times compared to the characteristic diffusion time t_D.

In the long-time limit (motion narrowing regime), the attenuation function in the impermeable sphere model contains not only terms linear in time, but also terms proportional to $t^{1/2}$, as in the case of permeable spheres; numerical coefficients are, however, different. The presence of $t^{1/2}$ terms can be important for correct interpretation of experimental data because the standard mono-exponential description of the signal in terms of the relaxation rate ΔR_2 (or ΔR_2^*) may not be adequate. In the cylindrical geometry, the leading term in the long-time expansion of the attenuation function is proportional to $t \ln t$ for both permeable and impermeable models also with different numerical coefficients.

Numerical (Monte–Carlo) simulations of the signal and comparison with its Gaussian approximation enabled us to deduce a validity criterion of the Gaussian approximation: $\zeta \cdot p = \zeta \cdot t_c/t_D > 1$, where ζ is the volume fraction of the magnetized inclusions, t_c and t_D are the characteristic dephasing and diffusion times, respectively.

Acknowledgments

The authors are grateful to Professors Mark S. Conradi and Joseph J.H. Ackerman for discussion and helpful comments. This work was supported in part by NIH Grants R01 NS41519, R01 HL7003701.

Appendix A. The correlation function for the impermeable cylinder model

Let us consider the diffusion equation in the space external to a cylinder of radius R. Introducing cylindrical coordinates (r,φ,z) with the polar axis z along the cylinder axis, the diffusion equation (6) for the propagator $P(\mathbf{r},\mathbf{r}_0,t)$ has the form

$$\frac{\partial P}{\partial t}=D\cdot\left[\frac{1}{r}\frac{\partial}{\partial r}\left(r\frac{\partial P}{\partial r}\right)+\frac{1}{r^2}\frac{\partial^2 P}{\partial\varphi^2}+\frac{\partial^2 P}{\partial z^2}\right] \tag{A.1}$$

with the initial condition $P(\mathbf{r},\mathbf{r}_0,0)=\delta(\mathbf{r}-\mathbf{r}_0)$ and boundary condition on the cylinder surface

$$\left(\frac{\partial P}{\partial r}\right)_{r=R}=0. \tag{A.2}$$

As diffusion along the cylinder axis is unrestricted, the solution of Eq. (A.1) can be factorized

$$P(r,\varphi,z;r_0,\varphi_0,z_0;t)=P_z(z,z_0,t)\cdot P_\perp(r,r_0;\varphi,\varphi_0;t), \tag{A.3}$$

where the factor $P_z(z,z_0,t)$ describes free diffusion along the z-axis

$$P_z(z,z_0,t)=\frac{1}{(4\pi Dt)^{1/2}}\exp\left[-\frac{(z-z_0)^2}{4Dt}\right] \tag{A.4}$$

and the function $P_\perp(r,r_0;\varphi,\varphi_0;t)$ describes restricted diffusion in the basal plane. The latter can be sought in the form:

$$P(r,r_0;\varphi,\varphi_0;t)=\sum_{m=-\infty}^{\infty}f_m(r,t)\exp(\mathrm{i}m\varphi), \tag{A.5}$$

where the functions $f_m(r,t)$ satisfy the equation

$$\frac{\partial f_m}{\partial t}=D\cdot\left[f_m''+\frac{1}{r}f_m'-\frac{m^2}{r^2}f_m\right],\quad f_m'(r=R,t)=0. \tag{A.6}$$

Hereafter an upper prime means a derivative with respect to the argument. Using the identity

$$\delta(\mathbf{r}-\mathbf{r}_0)=\frac{1}{r_0}\delta(r-r_0)\delta(\varphi-\varphi_0)\delta(z-z_0) \tag{A.7}$$

the initial condition of Eq. (A.6) can be written in the form

$$f_m(r,0)=\frac{\delta(r-r_0)}{2\pi r_0}\exp(-\mathrm{i}m\varphi_0). \tag{A.8}$$

The Laplace transformation of the function $f_m(r,t)$

$$\bar{f}_m(r,p)=\int_0^\infty \mathrm{d}t f_m(r,t)\exp(-pt), \tag{A.9}$$

satisfies the equation

$$p\bar{f}_m-D\cdot\left[\bar{f}_m''+\frac{1}{r}\bar{f}_m'-\frac{m^2}{r^2}\bar{f}_m\right]=\frac{\delta(r-r_0)}{2\pi r_0}\exp(-\mathrm{i}m\varphi_0). \tag{A.10}$$

A solution of Eq. (A.10) is a linear combination of the modified Bessel function $I_m(kr)$ and $K_m(kr)$ with $k=(p/D)^{1/2}$:

$$\bar{f}(r,p)=C_1I_m(kr)+C_2K_m(kr)+\frac{\exp(-\mathrm{i}m\varphi_0)}{2\pi D}\cdot\begin{cases}I_m(kr)K_m(kr_0), & r<r_0,\\ I_m(kr_0)K_m(kr), & r>r_0.\end{cases} \tag{A.11}$$

The coefficients C_1 and C_2 are determined by the boundary condition $\bar{f}_m'(r=R,p)=0$ and the finiteness condition at $r\to\infty$:

$$C_1=0,\quad C_2=-\frac{\exp(-\mathrm{i}m\varphi_0)}{2\pi D}\cdot\frac{K_m(kr_0)I_m'(kR)}{K_m'(kR)}. \tag{A.12}$$

Thus, the Laplace transformation of the function $P_\perp(r,r_0;\varphi,\varphi_0;t)$ takes the form:

$$\begin{aligned}\bar{P}_\perp(r,r_0;\varphi,\varphi_0;p)&=\sum_{m=-\infty}^{\infty}\bar{f}_m(r,p)\exp(\mathrm{i}m\varphi)\\&=\frac{1}{2\pi D}\sum_{m=-\infty}^{\infty}\exp(\mathrm{i}m(\varphi-\varphi_0))\\&\quad\cdot\left[\frac{K_m(kr_0)I_m'(kR)}{K_m'(kR)}K_m(kr)\right.\\&\quad\left.+\begin{cases}I_m(kr)K_m(kr_0), & r<r_0,\\ I_m(kr_0)K_m(kr), & r>r_0,\end{cases}\right].\end{aligned} \tag{A.13}$$

To calculate the correlation function $G(t)$, one should perform the inverse Laplace transformation of the function $\tilde{P}_\perp$ (A.13) and substitute the result in Eq. (4). However, it is more convenient to calculate first the Laplace transformation of the correlation function

$$\begin{aligned}\bar{G}(p)&=\int_0^\infty \mathrm{d}t\,G(t)\exp(-pt)\\&=\frac{1}{V_e}\left\langle\int\int\mathrm{d}\mathbf{r}_1\,\mathrm{d}\mathbf{r}_0\omega(\mathbf{r}_1)\omega(\mathbf{r}_0)\bar{P}(\mathbf{r}_1,\mathbf{r}_0,p)\right\rangle.\end{aligned} \tag{A.14}$$

Substituting Eq. (A.13) into Eq. (A.14) and using the explicit form of the magnetic field created by a magnetized cylinder

$$h(r,\varphi)=2\pi\Delta\chi H_0\sin^2\alpha\,\frac{R^2}{r^2}\cos 2\varphi,\quad r>R \tag{A.15}$$

(α is the angle between the cylinder's axis and the external field $\mathbf{H}_0$) the function $\bar{G}(p)$ can be written in the form

$$\begin{aligned}\bar{G}(p)=&\frac{45G_0R^2\langle\sin^4\alpha\rangle}{16D}\cdot\int_x^\infty\frac{\mathrm{d}y}{y}\int_x^\infty\frac{\mathrm{d}y_0}{y_0}\\&\times\left[\frac{K_2(y_0)K_2(y)I_2'(x)}{K_2'(x)}\right.\\&\left.+\theta(y_0-y)I_2(y)K_2(y_0)+\theta(y-y_0)I_2(y_0)K_2(y)\right],\end{aligned} \tag{A.16}$$

where G_0 is given in Eq. (10), $\theta(x)$ is the step-function, and a dimensionless variable $x = kR = (p/D)^{1/2}R$ is introduced. Besides, we took into account that

$$\int_0^{2\pi} d\varphi \int_0^{2\pi} d\varphi_0 \cos 2\varphi \cos 2\varphi_0 \exp[im(\varphi - \varphi_0)] = \begin{cases} \pi^2, & m = \pm 2, \\ 0, & m \neq \pm 2. \end{cases}$$

For the uniform distribution of the cylinder's orientation, the distribution function for α is $(\sin\alpha)/2$, $0 \leqslant \alpha \leqslant \pi$; hence, $\langle \sin^4 \alpha \rangle = 8/15$.

Performing integrations in Eq. (A.16) and using the identity

$$K_1(x)I_2'(x) + I_1(x)K_2'(x) = -\frac{2}{x^2},$$

we obtain

$$\bar{G}(p) = G_0 t_D \cdot q(x), \quad q(x) = \frac{3}{x^4}\left[\frac{K_1(x)}{K_2'(x)} + \frac{x^2}{2}\right]. \qquad (A.17)$$

For small and large argument, the function $q(x)$ can be approximated by

$$q(x) \simeq \begin{cases} 3(-\ln x - C + 1/2 + \ln 2)/8, & x \ll 1, \\ \frac{3}{4x^2}\left(1 - \frac{4}{x^2}\right), & x \gg 1. \end{cases} \qquad (A.18)$$

The correlation function $G(t)$ in the time-domain can be found by making use of the inverse Laplace transformation of $\bar{G}(p)$ (see Eq. (20) in the main text).

References

[1] A.L. Sukstanskii, D.A. Yablonskiy, Gaussian approximation in the theory of MR signal formation in the presence of structure-specific magnetic field inhomogeneities, J. Magn. Reson. 163 (2003) 236.

[2] A.L. Sukstanskii, D.A. Yablonskiy, Theory of FID NMR signal dephasing induced by mesoscopic magnetic field inhomogeneities in biological systems, J. Magn. Reson. 151 (2001) 107.

[3] Y. Ayant, E. Belorizky, J. Alizon, J. Gallice, Calcul des densites spectrales resultant d'un mouvement aleatoire de translation en relaxation par interaction dipolaire magnetique dans les liquides, J. de Phys. 36 (1975) 991.

[4] L.-P. Hwang, J.H. Freed, Dynamic effects of pair correlation functions on spin relaxation by translational diffusion in liquids, J. Chem. Phys. 63 (1975) 4017.

[5] S.C.-K. Chu, Y. Xu, J.A. Balschi, C.S. Springer, Bulk magnetic susceptibility shift in NMR studies of compartmentalized samples: use of paramagnetic reagents, Magn. Reson. Med. 13 (1990) 239.

[6] I.S. Gradstein, I.M. Ryzhik, Table of Integrals, Series, and Products, Academic Press, New York, 1999.

[7] J.H. Jensen, R. Chandra, NMR relaxation in tissues with weak magnetic inhomogeneities, Magn. Reson. Med. 44 (2000) 144.

[8] C.F. Hazlewood, D.C. Chang, B.L. Nichols, D.E. Woessner, Nuclear magnetic resonance transverse relaxation times of water protons in skeletal muscle, Biophys. J. 14 (1974) 583.

[9] S. Majumdar, J.C. Gore, Studies of diffusion in random fields produced by variations in susceptibility, J. Magn. Res. 78 (1988) 41.

[10] V.G. Kiselev, S. Posse, Analytical model of susceptibility-induced MR signal dephasing: effect of diffusion in a microvascular network, Magn. Reson. Med. 41 (1999) 499.

[11] D.W. Pfitsch, A.F. McDowell, M.S. Conradi, What are the conditions for exponential time-cubed echo decays?, J. Magn. Reson. 139 (1999) 364.

[12] P.P. Mitra, P.N. Sen, L.M. Schwartz, Short-time behavior of the diffusion coefficient as a geometrical probe of porous media, Phys. Rev. B 47 (1993) 8565.

[13] Y. Gossuin, P. Gillis, F. Lo Bue, Susceptibility-induced T(2)-shortening and unrestricted diffusion, Magn. Reson. Med. 47 (2002) 194.

[14] D.C. Douglass, D.W. McCall, Diffusion in paraffin hydrocarbons, J. Phys. Chem. 62 (1958) 1102.

[15] C.H. Neuman, Spin echo of spin diffusion in a bounded medium, J. Chem. Phys. 60 (1973) 4508.

[16] P.T. Callaghan, Principles of Nuclear Magnetic Resonance Microscopy, Claredon Press, Oxford, 1991.

[17] L.Z. Wang, A. Caprihan, E. Fukushima, The narrow-pulse criterion for pulsed-gradient spin-echo diffusion measurements, J. Magn. Res. A 117 (1995) 209.

[18] J. Stepisnik, Validity limits of Gaussian approximation in cumulant expansion for diffusion attenuation of spin echo, Physica B 270 (1999) 110.

[19] W.R. Bauer, W. Nadler, Spin dephasing in the extended strong collision approximation, Phys. Rev. E 65 (2002) 066123.

[20] A.L. Sukstanskii, D.A. Yablonskiy, Effects of restricted diffusion on MR signal formation, J. Magn. Reson. 157 (2002) 92.

[21] D.A. Yablonskiy, E.M. Haacke, Theory of NMR signal behavior in magnetically inhomogeneous tissues: the static dephasing regime, Magn. Reson. Med. 32 (1994) 749.

[22] C.V. Bowen, X. Zhang, G. Saab, P.J. Gareau, B.K. Rutt, Application of the static dephasing regime theory to superparamagnetic iron-oxide loaded cells, Magn. Reson. Med. 48 (2002) 52.

[23] R.M. Weisskoff, C.S. Zuo, J.L. Boxerman, B.R. Rosen, Microscopic susceptibility variation and transverse relaxation: theory and experiment, Magn. Reson. Med. 31 (1994) 601.

[24] J.L. Boxerman, L.M. Hamberg, B.R. Rosen, R.M. Weisskoff, MR contrast due to intravascular magnetic susceptibility perturbations, Magn. Reson. Med. 34 (1995) 555.

[25] W.M. Spees, D.A. Yablonskiy, M.C. Oswood, J.J.H. Ackerman, MR properties of human blood at 1.5 T. T1, T2, T2* and Gaussian relaxation behavior, Magn. Reson. Med. 45 (2001) 533.

[26] T. Shen, R. Weissleder, M. Papisov, A. Bogdanov, T.J. Brady, Monocrystalline iron oxide nanocompounds (MION): physicochemical properties, Magn. Reson. Med. 29 (1993) 599.

[27] C.W. Jung, P. Jacobs, Physical and chemical properties of superparamagnetic iron oxide MR contrast agents: ferumoxides, ferumoxtran, ferumoxsil, Magn. Reson. Imaging 13 (1995) 661.